Biogeosciences Discuss., 11, 4909–4947, 2014
www.biogeosciences-discuss.net/11/4909/2014/
doi:10.5194/bgd-11-4909-2014

Biogeosciences Discussions
Open Access

Chemical fate and settling of mineral dust in surface seawater after atmospheric deposition observed from dust seeding experiments in large mesocosms

K. Desboeufs[1], N. Leblond[2], T. Wagener[3], E. B. Nguyen[1], and C. Guieu[4,5]

[1]LISA, UMR CNRS 7583, Université Paris-Diderot et Université Paris-Est Créteil, 61, av du Général de Gaulles, Créteil, France
[2]Sorbonne Universités, UPMC Univ Paris 06, UMS 0829, Observatoire Océanologique, Villefranche-sur-Mer, France
[3]Université d'Aix-Marseille, CNRS/INSU, IRD, Institut Méditerranéen d'Océanologie (MIO), UM 110, 13288 Marseille, France
[4]Sorbonne Universités, UPMC Univ Paris 06, UMR 7093, LOV, Observatoire océanologique, 06230, Villefranche/mer, France
[5]CNRS, UMR 7093, LOV, Observatoire océanologique, 06230, Villefranche/mer, France

Received: 20 January 2014 – Accepted: 16 March 2014 – Published: 28 March 2014

Correspondence to: K. Desboeufs (desboeufs@lisa.u-pec.fr)

Published by Copernicus Publications on behalf of the European Geosciences Union.

Abstract

We report here the elemental composition of sinking particles in sediment traps and in the water column following 4 artificial mineral dust seedings (representing a flux of 10 g m^{-2}) in mesocosms, simulating dry or wet dust deposition into oligotrophic marine waters. These data were used to examine the rates and mechanisms of total mass, particulate organic carbon (POC) and elemental (Al, Ba, Ca, Co, Cu, Fe, K, Li, Mg, Mn, Mo, N, Nd, P, S, Sr and Ti) transfer from the surface to the sediment traps after dust deposition. The dust additions were carried out with fresh or artificially aged dust (i.e. enriched in nitrate and sulfate by mimicking cloud processing) for various biogeochemical conditions, enabling us to test the effect of these parameters on the chemical evolution and settling of dust after deposition. Whatever the type of seeding (using fresh dust to simulate dry deposition or artificially aged dust to simulate wet deposition), the dust was predominant in the particulate phase in the sediment traps at the bottom of mesocosms and within the water column during each experiment. 15 % of initial dust mass was dissolved in the water column in the first 24 h after seeding. For artificially aged dust, this released fraction was mainly nitrate, sulfate and calcium and hence represented a significant source of new N for the marine biota. Except for Ca, S and N, the elemental composition of dust particles was constant during their settling, showing the relevance of using interelemental ratios, such as Ti/Al or Ba/Al as proxy of lithogenic fluxes or of productivity. After 7 days, between 30 and 68 % of added dust was still in suspension in the mesocosms depending on the experiment. This difference in the dust settling was directly associated to a difference in POC export, since POC fluxes were highly correlated to dust lithogenic fluxes signifying a ballast effect of dust. The highest fraction of remaining dust in the mesocosm at the end of the experiment was found when the lowest chl *a* increase was observed, and inversely. This suggests a high interaction between a fertilizing effect of dust, a ballast effect, and POC fluxes. Our data emphasize a typical ratio Lithogenic/POC fluxes around 30 which could be used as reference to estimate the POC export triggered by wet dust deposition event.

BGD
11, 4909–4947, 2014

The elemental fluxes associated to the dust settling presented in this paper constitute also an original database on the export of atmospheric metals in a case of dry or wet dust deposition event.

1 Introduction

Dust particles deposition has been identified as a major source of main nutrients (Fe, N, P) for several oceanic regions (Jickells et al., 2005; Mahowald et al., 2008). Inversely, dust particle settling can be an efficient mechanism to remove dissolved nutrients from ocean surface waters, notably by adsorption onto sinking particles (e.g. Wagener et al., 2010). Thus, dust deposition plays a critical role on biogeochemical elemental cycling by acting as both a source and a sink of dissolved nutrients and trace metals in surface seawater. Indeed, chemical exchanges between dissolved elements and suspended and sinking particles drive, in concert with biological activities and oceanic circulation, the major chemical distributions of elements in seawater (e.g. Geotraces, 2006). A quantification of global dust deposition is essential for assessing the role of dust on the ocean realm. In particular, a quantification based on collected samples is crucial for the validation of dust transport models (Schulz et al., 2012). Also, the characterization of present-day dust deposition signatures may also be useful for the interpretation of the marine sedimentary records, since mineral dust is usually used as proxy of surface dryness and/or large-scale changes of circulation pattern (Skonieczny et al., 2011).

Atmospheric dust inputs to the ocean have been indirectly assessed from accumulation rates in sediments, and from sediment traps in the water column (e.g. Honjo et al., 2000). These marine-based methods are used to validate model outputs, assuming a conservative dust transfer through the water column. Sediment traps have also been used to quantify and characterize the atmospheric flux of elements from the surface to the deep sea (Buat-Menard et al., 1989; Buesseler et al., 1990). However, discrepancies are usually observed between dust and oceanic fluxes estimated from simultaneous measurements of dust fluxes by marine sediment traps and by atmo-

BGD
11, 4909–4947, 2014

spheric deposition method (Bory et al., 2002; Neuer et al., 2004). Various processes in the water column have been identified to explain these mismatches. Generally, dust considered as the lithogenic component must be isolated from the total flux of material mainly composed by biogenic minerals: opal and calcium carbonate, produced by organisms in the surface waters. This methodology is known to provide large uncertainties on the lithogenic fluxes (Buesseler et al., 2007). Moreover, the export of dust to the depth of the sediment traps is controlled by the ballast effect of organic matter produced by biological activity, and hence an efficient downward export of the dust particles to the sediment traps demands a biological activity (e.g. Bory et al., 2002; Fischer et al., 2009). Finally, dust particles can be horizontally advected or redistributed in the water column, before reaching the sediment trap.

The project DUNE (a DUst experiment in a low Nutrient low chlorophyll Ecosystem) aimed at better understanding the effect of dust deposition on the biogeochemistry of surface waters of the Mediterranean Sea (Guieu et al., 2010). The approach applied in this project was to perform dust addition experiments onto large clean mesocosms. The original design of these mesocosms represented unique opportunity to study the dust fate after deposition at the surface of a water column of 12.5 m, down to sediment traps. In particular, the use of mesocoms limits the problem of hydrodynamical artifact, i.e. later advection or losses of particles by stream, as observed for in situ sediment traps. In consequence, the DUNE experiments allowed assessing, in controlled conditions, the impact of dissolution, adsorption and chemical or biological process associated with the settling of particles in the surface water column.

Here we examine the source-to-sink transfer of added dust particles and the particles sorting by comparing the total mass and the elemental fluxes (POC, Al, Ba, Ca, Co, Cu, Fe, K, Li, Mg, Mn, Mo, N, Nd, P, S, Sr and Ti) of material collected in the traps. The suite of elements was chosen to include biological components (POC, Ca, Ba), elements associated with the dust addition (Al, Fe, Ca, Ti, N), elements that are major components of the flux (Si, Ca, Al, Mg, S) and elements that are minor components of the flux (P, trace metals: Mn, Cu, Co, Mo, Li and Nd). This paper presents the calcula-

BGD
11, 4909–4947, 2014

tion of POC and lithogenic fluxes which have been used to discuss the effect induced by dust deposition on the aggregation processes between organic material and dust (Bressac et al., 2013) and carbon budget (Guieu et al., 2013). The analysis of the behaviour of N released from dust presented in this work supports also the discussion of Ridame et al. (2013) on the N_2-fixation stimulated by dust deposition.

2 Materials and method

2.1 Dust seeding

The mesocosm experiment design and the accuracy of the strategy developed in the frame of the DUNE project are described in details in Guieu et al. (2010). In summary, the deployed mesocosms were cylindrical with 2.3 m in diameter and a 12.5 m height for the main cylindrical part. The bottom of the mesocosms was conical and a sediment trap collecting the exported material was adapted at the apex (at a depth of 15 m). The total volume of water in each mesocosm was 52 m^3 and the surface of mesocosms was 4.15 m^2. A system of permanent PVC tubing allowed sampling at three different depths (−0.1, −5 and −10 m) by connecting a Teflon pump. During the DUNE-R experiment, three additional sampling depth (−2.5, −7.5 and −12.5 m) have been added in two of the three mesocosms were the dust addition was performed. Mesocosms were covered in order to avoid possible additional inputs from natural dust events.

Two series of mesocosm seeding experiments happened at the beginning of summers 2008 and 2010: Experiments DUNE-P, DUNE-Q and DUNE-R (Table 1). The protocol of mesocosm deployment and dust seeding methodology are fully detailed in Guieu et al. (2010 and 2013). In brief, for these experiments, six (DUNE-P and Q) or seven (DUNE-R) mesocosms were deployed in the bay of Elbo (Scandola Marine preservation area −8.554° E, 42.374° N) during typical summer oligotrophic conditions. Three or four mesocosms (D1, D2, D3 and Dopt hereafter referred as “Dust-Meso”) were seeded with 41.5 g of dust – corresponding to a deposition flux of 10 g m^{-2} using

BGD
11, 4909–4947, 2014

a trace metal clean spray. The time of the dust addition corresponds to the theoretical start of the experiment (t_0). For the experiments DUNE-P and DUNE-R, the seeding simulated a wet deposition event by spraying diluted cloud processed dust (see Sect. 2.2) in 4 L of ultrapure water (Guieu et al., 2010). In the case of the experiment R, two consecutive seedings in the same mesocosms were carried out at the time t_0 then after 7 days, i.e. 164 h after the first seeding (first and second seedings, hereafter referred as Dune-R1 and DUNE-R2 respectively). For the experiment DUNE-Q, the seeding mimicked a dry deposition event by spraying diluted fresh dust in local seawater. In each experiment, three other mesocosms (C1, C2 and C3, hereafter referred as "Control-Meso") were kept unseeded for reference. The sediment traps screwed to the base of mesocoms at 15 m in depth were recovered and replaced by divers every 48 h for DUNE P and Q and every 24 h for DUNE-R.

2.2 Dust characteristics

The fine fraction < 20 µm in diameter of a dry sieved alluvial soil sample collected in a dust source area in southern Tunisia (33.452° N, 9.335° E) has been used to seed the mesocosms (Guieu et al., 2010). We used for seeding the fine fraction of soil as analog to Saharan aerosol particles (Desboeufs et al., 1999) in order to obtain enough quantity of the same material. Two campaigns of soil sampling have been made in March 2007 and March 2009 corresponding to sieved soil Dust07 and Dust09 respectively. The comparison of the physico-chemical properties of both soil samples (chemical and mineralogical composition and size distribution) indicate a good consistency (e.g. for chemical composition in Table 2), both samples being characterized by a large proportion of quartz (40 %) and calcite (30 %), then different clay minerals (25 %) as illite, kaolinite or palygorskite.

Saharan dust particles collected in Mediterranean atmosphere is usually mixed with organic and inorganic material, as sulfate or nitrate, due to cloud processing during atmospheric transport (e.g. Putaud et al., 2004). To reproduce this typical mixing effect in Mediterranean aerosols, we have artificially aged the soil sample by mimicking the

BGD
11, 4909–4947, 2014

pH gradients and the incorporation of inorganic and organic acid normally observed during cloud processing (Guieu et al., 2010). The soil treatment, i.e. sieving and cloud processing, has been made with the same procedure for the Dust07 and Dust09. The fine fraction of soil which underwent the protocol of cloud processing is noted EC-Dust for evapocondensed dust, and the fresh soil is noted NEC-Dust. The size distribution after treatment is similar with the one of fresh dust, i.e. a volume median diameter around 6.5 µm and a peak at ~ 10 µm (Guieu et al., 2010). The Table 1 presents the type of soils used for the 3 experiments. The effect of the simulated cloud processing on the formation of sulfate and nitrate at the surface of dust was checked by electronic microscope observations. This showed an enrichment of nitrogen and sulfur via the neoformation of evaporite mineral like gypsum (Fig. 1) consistent with the observations on the ageing of dust during atmospheric transport (e.g. Busek and Posfai, 1999). The enrichment in sulfur and nitrogen was also observed on elemental composition of EC-Dust07 and EC-Dust09 by X-ray spectrometry fluorescence analysis (Table 2). This enrichment is associated with a decrease in carbon content in the EC-Dust due to the reactions between calcite ($CaCO_3$) and inorganic acids to form the evaporite minerals, as gypsum ($CaSO_4$) or calcium nitrate ($Ca(NO_3)_2$), which release CO_2.

2.3 Chemical characterization of sediment trap samples

After recovery, the sample bottles of sediment traps were poisoned at 5 % with a solution of buffered formaldehyde to prevent microbial degradation and grazing by swimmers and were stored at 4 °C in the dark inside a refrigerator. The samples collected in the sediment trap were treated following the standard protocol developed at the national service "Cellule Piège" of the French INSU-CNRS. Swimmers were removed by hand-picking under the binocular microscope. The sample then underwent three rinses with 50 mL of ultrapure (MilliQ) water in order to remove salt and were then freeze-dried. Mass fluxes were measured by weighing five times the freeze-dried samples. The accuracy of the weighing was 1 % over the whole data series. Total concentration of carbon and nitrogen were measured in duplicate with a Perkin Elmer 2400 serie

BGD
11, 4909–4947, 2014

II elemental analyzer (CHN) on aliquots of the desiccated samples (3–4 mg). Acid digestion described by Ternon et al. (2010) was performed on aliquots (~ 15 mg) of the desiccated samples. The acid digestions of the sediment trap samples were carried out in parallel with referenced material (CRM GBW07313: marine sediment from NRC) in order to check the acid digestion protocol. Elemental composition was measured on digested samples after dilution (1/100) by Ametek ICP-AES for Al, Ca, Co, Cu, Fe, K, Li, Mg, Mn, Mo, Nd, P, S, Sr and Ti. The reliability of the digestion method was checked with a recovery for all the elements higher than 96 % in CRM samples. The accuracy of ICP-AES analyses was checked using SLRS-4 and SLRS-5 as CRM and the detection limits determined (Heimburger et al., 2013). Reagent blanks were included as control for possible contamination during the analytical process.

2.4 Particulate concentration in the water column

In order to follow both the settling of the added mineral particles through the mesocosms and the behaviour of particles during their settling, particulate concentrations for Al, Fe, Ca, Co, Cu, Fe, K, Li, Mg, Mn, Mo, Nd, P, S, Sr and Ti were measured in the water column during DUNE-R and only for Fe and Al during DUNE-P and DUNE-Q. The protocol used for sampling and treatment is described in Wagener et al. (2010). In brief, particulate samples were collected on 47 mm (pore size: 0.2 µm) cellulose acetate filters (Sartorius) previously washed by filtrating one litre of seawater. For the experiment P and Q, the samplings were operated at 0, 5 and 10 m at 6, 24, 46 and 70 h after seeding. For the R experiments, the samplings were operated in 5 depths in the mesocosms (0, 5, 7.5, 10 and 12.5 m) up to 164 h after seeding. After filtration, filters were dried under a laminar flow bench and kept at room temperature until analysis. One half of the collected filters were HNO_3/HF acid-digested then diluted in 10 mL of 0.1 M HNO_3 after complete evaporation. The obtained solutions were analyzed at LOV (Villefranche sur mer) for Al and Fe with a Jobin Yvon (JY 138 “Ultrace”) ICP-AES for DUNE-P and DUNE-Q (see Wagener et al., 2010). For DUNE-R, the digestion solutions were analysed at LISA (Créteil) by Ametek ICP-AES with the protocol used for

BGD
11, 4909–4947, 2014

the chemical characterization of sediments. For Co, Cu, Li, Mo and Nd, the measured concentrations were mainly under the limits of detections of this method. As the filters were not rinsed to remove salts, the data on Ca, K, Mg, S and Sr were highly affected by salts contained in the seawater and are not discussed here.

3 Results

3.1 Mass and elemental composition in sediment traps

The average total and elemental mass in the sediment traps for the 4 seeding experiments are presented in Table 3 for C, N, Al, Ca, S for the Control-Meso and Dust-Meso and in the Supplement section for Ba, Co, Cu, Fe, K, Li, Mg, Mn, Mo, Nd, P, Sr and Ti. The total and elemental masses were always higher in the Dust-Meso than in the Control-Meso, except for N in DUNE-Q.

On Fig. 2a, the cumulative total mass in the Dust-Meso sediment traps as a function of time is represented. For all experiments, the cumulative mass increased faster and was linear with the time in the first 90 h, then the mass increase was slower at the end of the experiments. Experiments DUNE-P and DUNE-R1 which happened in similar seeding conditions (Table 1 and Guieu et al., 2013) showed very similar variations of total mass in the sediment traps and presented the highest cumulated total mass. The maximum mass collected was reached between 24 h and 72 h for the experiment P and R1, whereas for the experiment R2 this maximum was obtained for the first trap samples, i.e. in the first 24 h (Table 3). The cumulated mass at the end of the experiment Q, mimicking dry deposition event, was one order of magnitude lower compared to the other experiments. In terms of chemical composition, C was the preponderant element in the sediment traps of Control-Meso, whereas Ca, C then Al were predominant in the sediment traps of Dust-Meso. This is consistent with the high content of these elements in the added dust (Table 2). The dominance of dust in the sediment traps for Dust-Meso was supported by the visible presence of dust in the samples after collection (Fig. 2b).

BGD
11, 4909–4947, 2014

The difference of elemental concentrations between the 4 experiments followed the variability of the total mass (Table 3), with the highest concentrations observed for the experiments P and R1 and the lowest for the experiments Q.

3.2 Elemental particulate concentrations in the water column

The distribution of particulate aluminium in the water column is presented for P, Q, R1 and R2 experiments in Fig. 3. The particulate concentrations of Ba, Fe, Mn, P, and Ti are given in Supplement. The vertical profiles of particulate Al and Fe for the experiment P are also described in Wagener et al. (2010). These data show that the particulate concentrations in Control-Meso were always lower to the ones found in Dust-Meso at a same depth. As lithogenic particles correspond mainly to added dust, particulate Al (pAl) was used as a tracer of this dust. Other studied elements followed the vertical profile of Al indicating their lithogenic origin. The highest pAl concentrations were observed in the first 5 m of mesocosms in the first 24 h for all the experiments (Fig. 3). For the experiments R, the pAl was mainly concentrated under 10 m after 48 h. These profiles of pAl stock for DUNE-R are in agreement with the optical measurements of Bressac et al. (2012) showing a sinking of dust particles under 10 m in the first 48 h after dust addition. A large part of the stock of pAl in DUNE-R2 remained concentrated in surface until 72 h whereas the stock of pAl presented a most homogeneous distribution in the water column for DUNE-R1. This is consistent with the difference in settling of particles observed from masses collected in sediment traps between DUNE-R1 and DUNE-R2. Thus, the sinking of dust was slower in DUNE-R2 in comparison to DUNE-R1. 164 h after the seeding, the pAl concentrations were always higher in Dust-Meso than in Control-Meso (not shown). This means that the addition of dust in the mesocosms triggered an increase of particulate concentrations on the water column even 7 days after seeding. No measurement of pAl was available at 2.5, 7.5 and 10 m below the surface for the experiments P and Q, limiting the conclusions on the location of added dust. However, the low total mass found in the sediment traps and the similar

BGD
11, 4909–4947, 2014

behaviour of dust settling in the first 24 h to the other experiments suggest potential high concentration of pAl in the water column even at the end of the experiment.

4 Discussion

4.1 Chemical evolution of dust during settling

For most elements, it appears that the elemental mass concentrations were linearly correlated with the total mass with a correlation coefficient higher than 0.98, except for N which presented a largest dispersion (Al and N are shown in Fig. 4). The linearity of scatter plot implies that the sediment composition was quasi-constant from 24 h after seeding up to the end of the experiment (168 h or 172 h after seeding), showing that the chemical composition of sinking particles collected in sediment traps did not evolve after the first 24 h during an experiment. In consequence, this linearity means that the process likely involved in a modification of composition (such as dissolution, adsorption, precipitation, aggregation) occurred in the water column before t = 24 h after the seeding, confirming that the study of these processes demands a high temporal resolution of dissolved concentrations monitoring as observed by Wuttig et al. (2013).

From the chemical composition of particles in the sediment traps, we tried to estimate the part issued from dust and from biological particles. Dissolved Al measurements in the water column during R experiments showed that this element presents a low fractional solubility ranging from 0.74 % to 0.84 % (Wuttig et al., 2013). In order to compare the composition of added mineral dust and of the particles collected in the sediment traps, we used the elemental concentration ratio of X/Al in sediment traps normalized to the X/Al ratio in dust (Table 4). Doing this, we identified enrichment or depletion of elements X independently of total mass variations. No significant evolution of Ba, Fe, Ti, Nd, Mo and Li contents was observed between added dust and collected particles in the Dust-Meso sediment traps. This confirms that their presence was associated to the dust sinking, in agreement with the observations in the water column. In contrast,

BGD
11, 4909–4947, 2014

for C, Co, Cu and K, the results show a systematic enrichment whatever the experiment, suggesting a supplementary biological source of these elements. Inversely, an important depletion of Ca and S was also observed. The behaviour of some other elements was contrasted depending on the experiments. This is the case for N and P which were highly enriched in the sediment traps in comparison to the added dust in DUNE-Q, carried out with NEC-Dust07 whereas N was depleted in DUNE-P and DUNE-R, seeded with EC-Dust. Thus, P was mainly associated to the dust sinking for the experiments DUNE-P and DUNE-R but affected by biological source in the case of DUNE-Q. Regarding the depletion of Ca, N, S, they are the major constituents of evaporites minerals as gypsum ($CaSO_4$) or calcium nitrate ($Ca(NO_3)_2$) which has been formed by cloud processing into EC-Dust. These minerals are known to be water soluble material (Sullivan et al., 2007). Moreover, dissolution experiments performed in laboratory on EC-Dust07 showed that 100 % of N, associated with the neoformation of calcium nitrate was dissolved as nitrate in seawater (Ridame et al., 2013). Thus, the depletion of Ca, S and N was probably due to the dissolution of sulfate and nitrate containing-particles into seawater after seeding. Moreover, the depletion was observed for all the samples whatever the time after seeding (not shown), confirming that this dissolution happened during the first 24 h. The dissolution of calcium nitrate represented a release of about 500 mg of dissolved nitrogen in the mesocosms for the experiments P, R1 and R2. This dissolution happened in the first 24 h, i.e. when dust was located in the upper 5 m of mesocosms (see 3.2 and Bressac et al., 2012). On this base (about 500 mg in the upper 5 m), we estimated that the N and NO_3^- dissolved concentrations were around 9 mmol m^{-2} or 40 mmol m^{-2} at 24 h, respectively. These data are in agreement with the measured NO_3 concentrations (11 mmol m^{-2}) in the mesocosms during R experiments (Ridame et al., 2014), confirming the large dissolution of evaporite minerals after the dust seeding. The two known sources of new nitrogen to the ocean are N_2 fixation and atmospheric deposition, mainly anthropogenic nitrogen aerosols deposition (de Leeuw et al., 2013). Our results suggest that the ageing of dust by HNO_3 uptake during its transport in the atmosphere could be also a potential major source

BGD
11, 4909–4947, 2014

of external dissolved N to the marine biosphere after dust deposition. On the contrary, when the seeding was carried out by NEC-Dust in DUNE-Q, an enrichment of N by a factor 7 was observed in the traps, suggesting another process, possibly a biological source. During this experiment, the N cumulative masses found in the sediment traps of the Dust-Meso were not significantly different from the ones in the Control-meso (Table 3). This means that this enrichment is mainly due to the biota initially present in the mesocosm and is consistent with the fact that no significant chlorophyll *a* (Chl *a*) increase has been observed for DUNE-Q after dust addition (Guieu et al., 2013). Ridame et al. (2014) show the dry deposition of dust during experiment Q led to a strong increase of N_2 fixation by diazotrophs. They estimated that this new nitrogen represents 50.4 µmolN m^{-2} in the Dust-Meso. Our data show that this new N was not exported in the sediment traps in the 7 days of the experiment. In the case of DUNE-P and DUNE-R, the enrichment of settling particles in N was not significant in comparison to the loss of N by dissolution and the input of P by the dust settling (dust mass from sediment traps is 10-fold higher than in DUNE-Q), preventing the observation in settling particles of N and P related to the biological source.

Practically, the interelemental ratios found in sediments are usually used as proxies of terrigenous input (Ti/Al, Fe/Ca and Ti/Ca) (Mahiques et al., 2009; Govin et al., 2012), and of productivity (Ba/Al and Ba/Ti) (Paytan and Kastner, 1996; Mahiques et al., 2009). Recent studies show that the potential of elemental ratios including Ca as Fe/Ca or Ti/Ca are too sensitive to dilution effects by biological components to allow reliable imprints of terrigeneous inputs (Govin et al., 2012). Our data support this conclusion by showing that the high solubility of Ca in dust creates a depletion of particulate Ca content during the settling of dust, which increases the Fe/Ca and Ti/Ca ratios in particles. Thus, the dissolution effect is combined to the dilution by organic matter effect making difficult to use these ratios for estimate lithogenic fluxes. On the contrary, our results show the stability of Al, Ba, Fe and Ti content in dust during their sinking in the water column, confirming the reliable use of their interelemental ratios as terrigeneous and productivity proxies.

BGD
11, 4909–4947, 2014

4.2 Mass budget in the sediment traps

A current method to estimate the total fluxes of dust in sediment traps is to use the Al content of lithogenic particles (Bory et al., 2002). Here, using the Al mass fraction to estimate the dust mass in the sediment traps, we found higher estimated dust mass than measured total mass (Table 5). The low fractional solubility observed for Al (see Sect. 4.1.) implies that the Al content in dust stayed constant during settling, and hence cannot explain the overestimation of mass between estimation using Al and actual measurement. Linear regression between total mass and elemental mass enables to estimate the % of a given element in the sediment traps. For instance, in Fig. 4, it appears that Al is 4.82 ± 0.12 % of the total mass for DUNE-P, a value significantly higher than the initial Al mass fraction in the seeded dust (4.12 ± 0.39 %, Table 1). This overestimation of mass percentage is also observed for all the other studied elements except Ca, S and N. For these three elements, the mass fractions are significantly lower in the sediment traps than in the added dust, in agreement with the dissolution of evaporite minerals.

Based on the assumption that the depletion of N and S in the sediment traps is due to the dissolution of $CaSO_4$ and $Ca(NO_3)_2$, we could assess the mass of seeded dust that dissolved except for the experiment Q (Table 5). In the case of the DUNE-Q, the estimated mass from Al is lower that the measured total mass. However, a loss of Ca is observed between the theoretical Ca mass (estimated from dust mass content of Ca) and the value which is measured in the trap samples. In consequence, we considered a potential dissolution of $CaCO_3$, the major material containing Ca in NEC-Dust07. So, for DUNE-Q, we used the Ca content in sediment traps to estimate the dissolved part, considering that all the depletion of Ca is associated to the dissolution of calcium carbonate (Table 5). On this basis of calculations, it appears that the dissolution of dust constituted a mass loss of around 7 g in each experiment i.e. that only about 34 g of dust from the seeded 41.5 g remained under particulate form in the mesocosms. If we compare the total mass measured in the sediment traps and the estimated mass of

BGD
11, 4909–4947, 2014

particulate dust considering dissolution (Table 5), it appears that the large majority of total mass was due to dust settling. However, the dust fraction represented only 75 % of total mass for DUNE-Q simulating a dry deposition whereas it was more than 97 % for the other experiments simulating wet deposition. This means a difference of dust settling in the two seeding protocols.

The estimated dust mass fraction recovered in the sediment traps is presented as a function of time in Fig. 5. It appears that a large part of the introduced dust was not recovered in the sediments traps even after taking account of the dissolution. This is consistent with our data on pAl concentrations in the water column and the results of Bressac et al. (2012), which showed by optical measurements that in spite of a very rapid dust settling in the first hours after seeding, a part of dust still remained in suspension 2 days after seeding for DUNE-R. Our data seem to show that it was still the case even 7 days after seeding, since only 52 %, 11 %, 57 % and 41 % by mass of the lithogenic particles initially added were recovered in the sediment traps in P, Q, R1 and R2 seedings, respectively (Fig. 5). For the experiments P and R with EC-Dust, the temporal evolution of dust settling was very homogeneous up to 72 h. Then the settling of lithogenic particles in the experiment R2 was significantly slowed down in comparison to the experiments P and R1. This pattern explains the difference of dust mass observed in the sediments traps at the end of the experiments. The low recovery of dust mass in the sediment traps even 7 days after seeding suggests that more than 45 % of dust particles (Fig. 5) had sinking velocities inferior to 2.1 $m\,d^{-1}$, whereas the recovery after one day indicates that less than 15 % of dust presented sinking velocities superior to 14.7 $m\,d^{-1}$ for DUNE-P and DUNE-R. This is consistent with the results of Bressac et al. (2012) which showed that the most rapid settling velocity of Saharan dust pool could reach 24 to 87 $m\,d^{-1}$ during DUNE-R. These high velocities correspond to the formation of organic-mineral aggregates within the upper few meters of the water column after seeding (Bressac et al., 2012). However, only a part of dust seems to form aggregates (Bressac et al., 2012). The lowest measured velocities could be explained by the fine size distribution of seeded dust which presents a volume median diameter

BGD
11, 4909–4947, 2014

of about 6.5 µm. For DUNE-Q, these percentages reached 89 % of particles with sinking velocities inferior to 2.1 m d^{-1}, and 1 % of particles with sinking velocities superior to 14.7 m d^{-1} (Fig. 5). This means that the large majority of deposited dust remained in the water surface layer even 7 days after the dry event.

Then, from the mass budget found from the sediment traps and from pAl concentration in the water column, we made the total mass budget of dust integrated from the surface to the sediment traps. We further used the estimated content of Al in the sediments traps from the Fig. 4 (top) compared to the initial content in seeded dust, in order to consider also the dissolution of dust particles during their settling. The results show that the total mass of dust in the mesocosms was 33.3 g, 11.6 g, 33.7 g and 26.9 g respectively for the experiments P after 5 days, Q after 3 days, R1 and R2 after 6 days (these times corresponding to the last sampling in the water column). Thus, considering the dissolved mass fraction from dust, we found a recovery of 96 %, 28 %, 99 % and 82 % of the initial dust mass, a half of which was in the sediment traps for DUNE-Q and DUNE-R2 and 2/3 for DUNE-P and DUNE-R1. A critical point of uncertainties in this calculation is the integration of pAl within the water column to estimate the mass of dust in suspension. As previously discussed, no measurement of pAl was available under 10 m for P and Q experiments whereas potential high concentration of pAl could be present at these depths. Thus, it is probable that this low depth resolution was insufficient for the case of the Q experiment, which presented the largest mass fraction in suspension at the end of the experiment, and hence this could explained, at least in part, the low rate of recovery for this experiment.

4.3 Estimation of fluxes associated to dust deposition

Results show that the temporal pattern of sinking of particles was not equivalent for all the experiments, with a much slower settling observed for DUNE-Q, simulating dry deposition of dust, and the highest being observed for DUNE-P and DUNE-R1. Settling particles consist of four major components: biogenic opal (opal), biogenic carbonate ($bCaCO_3$), lithogenic particles, and organic matter (POC). In the Dust-Meso,

BGD
11, 4909–4947, 2014

the lithogenic particles corresponded essentially to added dust. In consequence, the fraction of dust was calculated from the estimated mass% of Al in the sediments traps from the Fig. 4, as for the mass budget. The fraction corresponding to biogenic opal was determined from the measurement of biogenic Si, issued from sequential leaching (Mosseri et al., 2005). In comparison to usual sediment traps studies, we know that a large part of Ca measured in the traps was issued from added dust. Thus, the total mass of Ca is the sum of Ca as $Ca(NO_3)_2$, $CaCO_3$ and $CaSO_4$ present in dust, plus the $bCaCO_3$. The observations of S concentration in the trap showed that all the produced gypsum by dust treatment was not completely dissolved. The undissolved mass of $CaSO_4$ was estimated from the mass of particulate S. The total carbonate mass was so assessed from the total mass of Ca minus the mass of Ca related to gypsum. The biogenic carbonate was finally estimated from the total carbonate mass minus the estimated $CaCO_3$ issued from dust (estimated from the Ca to total mass scatter plot as for Al in Fig. 4). The organic matter was estimated as 2.4 times the organic carbon (Klaas and Archer, 2002), which was issued from the total carbon mass less the total carbonate fraction of carbon.

On this basis, we have estimated the part of various fractions in the sediments traps. The masses in the Control-Meso were typically at least one order of magnitude inferior to the masses obtained in the Dust-Meso. The Control-Meso were dominated by the POC fraction (30 to 50 %), then by the lithogenic fraction (20–30 %) whatever the experiment. Inversely, the lithogenic fraction was the main component of the mass in the Dust-Meso, representing between 66 to 96 % of total mass with the lowest percentages measured from 6 days after seeding (not shown). The fraction of POC represented up to 14 % of the total mass. The highest POC concentrations were obtained for the experiment P whereas the lowest for the experiment Q. From these data, the total mass flux, POC flux and the fluxes of many elements have been estimated from the mass concentration and fraction in sediment traps (Tables 6 and 7). All the fluxes were significantly lower in the experiment Q than in the other experiments, in agreement with the low dust recovery found in the sediment traps of this seeding. The data will be

BGD
11, 4909–4947, 2014

discussed here by comparing the integrated POC fluxes between the various experiments, a discussion on the POC evolution as a function of time is presented in Bressac et al. (2013) for the R experiments.

The total and lithogenic fluxes obtained for DUNE-P and DUNE-R (Table 6) are higher than typical fluxes observed in regions under dust deposition influence, typically around 50 $mg\,m^{-2}\,d^{-1}$ (Bory et al., 2002 for Northeastern tropical Atlantic Ocean; Ternon et al., 2010 for Western Mediterranean). However, our data are consistent with the observed lithogenic fluxes after a large dust event (22 $g\,m^{-2}$) in Mediterranean reaching 1 $g\,m^{-2}\,d^{-1}$ at 200 m (Ternon et al., 2010). In the same way, the POC fluxes (10–20 $mg\,m^{-2}\,d^{-1}$) are consistent with typical POC fluxes measured in Western Mediterranean (Miquel et al., 1994; Goutx et al., 2000; Lee et al., 2009; Ternon et al., 2010). Contrary to major fractions, little information is available on the elemental fluxes associated to a large dust wet deposition event. As the lithogenic fraction predominates in all the Dust-Meso sediment traps for the different experiments, most elemental fluxes correspond to the content of these various elements in the added dust. Our measured fluxes of trace metals (Table 7) constitute so an original assessment of the fate of the atmospheric input of these metals in a marine environment. This database could enable us to distinguish the contribution of dust and other sources, e.g. anthropogenic, in the biogeochemical cycling of these elements. Moreover, the typical comparison between atmospheric and marine dust fluxes estimated from Al contents shows that estimated atmospheric deposition fluxes are 2–3 times lower than oceanic sediment trap fluxes (Bory et al., 2002; Ternon et al., 2010). Here, in very controlled conditions, we observed that the estimation of dust mass from Al is on average 30 % larger than the real added mass of dust. As mentioned before, Al is often used for estimating the dust mass in sediment traps (e.g. Bory et al., 2002). Our results show that the dissolution of evaporite minerals formed during atmospheric dust transport due to cloud processing could generate an overestimation of the dust total mass estimated like that. This suggests that the uncertainties on the estimation of lithogenic fluxes from Al content in sediment traps could be very largely higher than 100 %.

BGD
11, 4909–4947, 2014

From observations during experiments R, Bressac et al. (2013) propose a ballast effect of added dust on the organic matter present in the mesocosms to explain the high degree of covariance between POC and lithogenic fluxes in the Dust-Meso. We observed that the positive covariance between lithogenic and POC fluxes exists also for the experiments P and Q. In order to estimate the efficiency of dust settling to ballasting organic matter as POC, we estimated the mass ratios of lithogenic matter (= dust in the Dust-Meso) to organic carbon in the sediments traps (Litho/POC in Table 6), i.e. dust fluxes normalized to the POC fluxes. The obtained mean ratios are around 30, in the range of values found in the case of "real" wet dust deposition events into surface seawater with high organic matter concentrations (Ternon et al., 2010). In the same way, the lowest ratio (13) obtained for the experiment Q corresponding to a dry deposition is consistent with the ratio observed by Ternon et al. (2010) in Mediterranean summer conditions with a strong stratification of the water column and low Chl *a* concentrations. To explain these different behaviours between dust and POC fluxes, it is important to consider the difference of seeding protocol simulating wet or dry deposition (Table 1), but also the physical and biogeochemical conditions in the 4 experiments (Guieu et al., 2010 and 2013). During the experiment P, the stratification of the column water inside the mesocosms was not marked whereas stratification was observed during the whole DUNE-Q experiment and toward the ends of both R-seeding periods. However, the dust settling is quasi-similar for DUNE-P and DUNE-R1, meaning that the stratification effect is probably low. Moreover, initial biogeochemical conditions were typical of oligotrophic conditions for all the experiments with very low Chl *a* concentrations in the range 0.07–0.11 $\mu g L^{-1}$ (Ridame et al., 2014). The chlorophyll concentration was at least doubled for DUNE-P and DUNE-R, proving a fertilizing effect of dust on phytoplankton (Ridame et al., 2014). Inversely, no Chl *a* increase was observed after seeding in the Q experiment. It is known that dust affects biogeochemical processes in marine environment via both a fertilizing role for marine biota (Bishop et al., 2002) and a ballast effect for POC export (Fischer et al., 2009), the ballast effect increasing the sinking velocity of particles (Ploug et al., 2008). Moreover, it has been suggested that the high lithogenic fluxes

BGD
11, 4909–4947, 2014

associated to dust deposition occur only when there is simultaneous presence of organic matter and lithogenic material (Ternon et al., 2010). This organic matter could be freshly produced due to a fertilizing effect of deposited dust or older. Our results confirm these previous observations by showing that the highest POC and lithogenic fluxes are observed when an increase of chlorophyll concentrations is observed. On the contrary, the observations for the experiment Q simulating dry dust deposition show a slower dust settling and a low POC export related to an ineffective fertilizing effect for primary productivity. Thus, ballasting from dust resulted in 4-fold higher POC fluxes in presence of phytoplankton than without Chl *a*. This observed primary-productivity dependence of lithogenic fluxes in our controlled oligotrophic conditions shows that a high POC export related to dust event needs both a fertilizing effect and mineral ballast of dust seeding. The high covariance observed between lithogenic and POC fluxes is similar for all the experiments simulating wet deposition, suggesting that the measured ratio Lithogenic/POC fluxes around 30 (Table 6) could be used as reference to estimate the POC export triggered by wet dust deposition event.

Recently, Bressac and Guieu (2013) defined the "lithogenic carbon pump" to describe the relation between the lithogenic ballasting and POC export, independently of the biological contribution to POC export. They suggest that the age and quantity of organic matter could be also essential to estimate the efficiency of the "lithogenic carbon pump". From this concept, Bressac et al. (2013) show that this lithogenic carbon pump represented 50 ± 8 and 42 ± 3 % of the POC fluxes after the DUNE-R1 and DUNE-R2 seeding, respectively. They propose that the relative decrease in the lithogenic ballasting after the second seeding is due to the scavenging of most of the biogenic particles from the water column following the first seeding. Comparing these conclusions with our observations on the POC fluxes during P and Q experiments suggests that the "lithogenic carbon pump" is inefficient for DUNE-Q since the POC fluxes in the Dust-Meso were similar with the ones in the Control-Meso. This implies that the initial organic matter presented probably a too low concentration or an inappropriate quality (e.g. thickiness) to induce a lithogenic ballasting in this experiment, whereas

BGD
11, 4909–4947, 2014

the fertilizing effect associated to the experiments P and R is able to produce sufficient fresh organic matter to activate the lithogenic carbon pump. Thus, our results suggest that the "lithogenic carbon pump" due to dust deposition needs probably to be associated with a fertilizing effect to be efficient when initial organic matter is insufficient or inefficient to be adsorbed on dust.

5 Conclusion

Determination of elemental particulate composition in sediment traps and along the water column in mesocosms constitutes useful data for assessing the evolution of dust particles after their deposition into seawater and the associated fluxes. Our measurements showed that the dust predominated the particulate phase in sediment traps at the bottom of mesocosms (15 m depth) and that dust particles were still in the 15 m water column after 164 h. The measured lithogenic and POC fluxes in mesocosms were consistent with direct observed fluxes in the water column after dust deposition (Ternon et al., 2010), confirming that our data were representative of the mechanisms of export after dust deposition event. Besides elemental fluxes usually estimated, e.g. Al, Ba or Ca (Winkler et al., 2005), the suite of elements analysed in the sediment traps enabled us to obtain a database on the fluxes of several trace elements which constitutes original measurements on atmospheric metals fluxes associated to dry and wet dust deposition.

Comparing the recovery of initial added dust mass in the sediment traps reveals a difference in the dust settling of dust between the various seeding experiments. A high recovery rate of dust mass (82 to 99 %) along the water column measured in DUNE-P and DUNE-R was associated to the highest POC and lithogenic fluxes. This corresponded to the seeding experiments carried out with EC-Dust, i.e. "aged" dust and simulating wet deposition, when a significant Chl *a* increase was observed. Inversely, the experiment Q, simulating a dry deposition event of NEC-Dust, i.e. "fresh" dust, presented the lowest recovery of dust mass in the sediment traps, with around 89 % of

BGD
11, 4909–4947, 2014

dust remaining in the water column after 6 days. This low sinking velocity involved a low POC export in association with a low Chl *a* increase during this experiment. Our data imply that being inefficient to fertilize mesocosms, the dry deposition of fresh dust in our oligotrophic conditions is inefficient to trigger a high POC fluxes by a ballast effect. On the contrary, they point the efficiency to the wet deposition of aged dust to imply a high POC fluxes associated to its fertilizing effect. In this case, the results show that the lithogenic fluxes were typically 30-fold higher than the POC fluxes. Thus, our data emphasize a chain reaction between the fertilizing effect of dust, their ballast effect and POC fluxes. However, our data do not enable to conclude if the type of deposition (dry or wet) is a critical parameter in this relation due to the difference in used dust between the experiments simulating dry or wet deposition.

Moreover, our results show that about 15 % of initial dust mass was dissolved in the water column in the first 24 h after seeding. This loss of mass was associated to the depletion of Ca, N and S in the dust recovered in the sediment traps, which was due to the rapid dissolution of calcite for DUNE-Q and from the new minerals, as gypsum or calcium nitrate formed by artificial cloud processing of seeded dust in DUNE-P and DUNE-R. This dissolution constitutes an important source of dissolved nitrate in the seawater, suggesting the potential importance of atmospheric deposition of "aged" dust as source of new N for oligotrophic area. In spite of this dissolution, the typical interelemental ratio, as Ti/Al or Ba/Al were not affected during the dust settling, confirming their interest as proxy of lithogenic fluxes or of productivity, respectively.

Supplementary material related to this article is available online at http://www.biogeosciences-discuss.net/11/4909/2014/bgd-11-4909-2014-supplement.zip.

Acknowledgements. The DUNE project, a DUst experiment in a low Nutrient, low chlorophyll Ecosystem, is a fundamental research project funded by the ANR under the contract "ANR-07-BLAN-0126-01". DUNE was endorsed by the international SOLAS (Surface Ocean–Lower

BGD
11, 4909–4947, 2014

Atmosphere) program in February 2009, (http://solas-int.org/activities/project-endorsement.html). The sediment trap treatments have been performed by the national service "La Cellule Pièges" from INSU LEFE-CYBER (L. Coppola, N. Leblond). The soil dust samples have been obtained from F. Dulac in collaboration with M. Labiadh from the Tunisian Institute of Arid regions (IRA) in Medenine.

References

Bishop, J. K. B., Davis, R. E., and Sherman, J. T.: Robotic observations of dust storm enhancement of carbon biomass in the North Pacific, Science, 298, 817–821, 2002.

Bory, A., Dulac, F., Moulin, C., Chiapello, I., Newton, P. P., Guelle, W., Lambert, C. E., and Bergametti, G.: Atmospheric and oceanic dust fluxes in the northeastern tropical Atlantic Ocean: how close a coupling?, Ann. Geophys., 20, 2067–2076, doi:10.5194/angeo-20-2067-2002, 2002.

Bressac, M., Guieu, C., Doxaran, D., Bourrin, F., Obolensky, G., and Grisoni, J. M.: A mesocosm experiment coupled with optical measurements to assess the fate and sinking of atmospheric particles in clear oligotrophic waters, Geochem. Mar. Letters, 32, 153–164, 2012.

Bressac, M., Guieu, C., Doxaran, D., Bourrin, F., Desboeufs, K., Leblond, N., and Ridame, C.: Quantification of the lithogenic carbon pump following a dust deposition event, Biogeosciences Discuss., 10, 13639–13677, doi:10.5194/bgd-10-13639-2013, 2013.

Buat-Menard, P., Davies, J., Remoudaki, E., Miquel, J. C., Bergametti, G., Lambert, C. E., Ezat, U., Quetel, C., La Rosa, J., and Fowler, S. W.: Non-steady-state biological removal of atmospheric particles from Mediterranean surface waters, Nature, 340, 131–134, 1989.

Buesseler, K. O., Livingston, H. D., Honjo, S., Hay, B. J., Konuk, T., and Kempe, S.: Scavenging and particle deposition in the southwestern Black Sea – evidence from Chernobyl radiotracers, Deep-Sea Res., 37, 413–430, 1990.

Buesseler, K. O., Antia, A. N., Chen, M., Fowler, S. W., Gardner, W. D., Gustafsson, O., Harada, K., Michaels, A. F., Van der Loeff'o, M. R., Sarin, M., Steinberg, D. K., and Trull, T.: An assessment of the use of sediment traps for estimating upper ocean particle fluxes, J. Mar. Res., 65, 345–416, 2007.

BGD
11, 4909–4947, 2014

Buseck, P. R. and Posfai, M. L.: Airborne minerals and related aerosol particles: effects on climate and the environment, P. Natl. Acad. Sci. USA, 96, 3372–3379, doi:10.1073/pnas.96.7.3372, 1999.

de Leeuw, G., Guieu, C., Arneth, A., Bellouin, N., Bopp, L., Boyd, P., Gon, H. C. D., Desboeufs, K., Dulac, F., Facchini, M. C., Gantt, B., Langmann, B., Mahowald, N., Maranon, E., O'Dowd, C., Olgun, N., Pulido-Villena, E., Rinaldi, M., Stephanou, E., and Wagener, T.: Ocean–atmosphere interactions of particles, in: Ocean–Atmosphere Interactions of Gases and Particles, Springer Earth System Sciences, Springer, Berlin, Heidelberg, 171–246, 2013.

Desboeufs, K., Losno, R., Vimeux, F., and Cholbi, S.: pH dependent dissolution of wind transported Saharan dust, J. Geophys. Res., 104, 21287–21299, 1999.

Fischer, G., Karakas, G., Blaas, M., Ratmeyer, V., Nowald, N., Schlitzer, R., Helmke, P., Davenport, R., Donner, B., Neuer, S., and Wefer, G.: Mineral ballast and particle settling rates in the coastal upwelling system off NW Africa and the South Atlantic, Int. J. Earth Sci., 98, 281–298, doi:10.1007/s00531-007-0234-7, 2009.

GEOTRACES Planning Group: GEOTRACES Science Plan, Scientific Committee on Oceanic Research, Baltimore, Maryland, 2006.

Goutx, M., Momzikoff, M., Striby, L., Andersen, V., Marty, J.-C., and Vescovali, I.: High-frequency fluxes of labile compounds in the central Ligurian Sea, northwestern Mediterranean, Deep-Sea Res. Pt. I, 47, 533–556, 2000.

Govin, A., Holzwarth, U., Heslop, D., Ford Keeling, L., Zabel, M., Mulitza, S., Collins, J. A., and Chiessi, C. M.: Distribution of major elements in Atlantic surface sediments (36° N; 49° S): imprint of terrigenous input and continental weathering, Geochem. Geophy. Geosy., 13, Q01013, doi:10.1029/2011gc003785, 2012.

Guieu, C., Dulac, F., Desboeufs, K., Wagener, T., Pulido-Villena, E., Grisoni, J.-M., Louis, F., Ridame, C., Blain, S., Brunet, C., Bon Nguyen, E., Tran, S., Labiadh, M., and Dominici, J.-M.: Large clean mesocosms and simulated dust deposition: a new methodology to investigate responses of marine oligotrophic ecosystems to atmospheric inputs, Biogeosciences, 7, 2765–2784, doi:10.5194/bg-7-2765-2010, 2010.

Guieu, C., Ridame, C., Pulido-Villena, E., Bressac, M., Desboeufs, K., and Dulac, F.: Dust deposition in an oligotrophic marine environment: impact on the carbon budget, Biogeosciences Discuss., 11, 1707–1738, doi:10.5194/bgd-11-1707-2014, 2014.

BGD
11, 4909–4947, 2014

Guieu, C., Dulac, F., Ridame, C., and Pondaven, P.: Introduction to project DUNE, a DUst experiment in a low Nutrient, low chlorophyll Ecosystem, Biogeosciences, 11, 425–442, doi:10.5194/bg-11-425-2014, 2014.

Heimburger, A., Tharaud, M., Monna, F., Losno, R., Desboeufs, K., and Nguyen, E.: SLRS-5 Elemental concentrations of thirty-three uncertified elements deduced from SLRS-5/SLRS-4 ratios, Geostand. Geoanal. Res., 37, 77–85, doi:10.1111/j.1751-908X.2012.00185.x, 2013.

Honjo, S., François, R., Manganini, S. J., Dymond, J., and Collier, R.: Particle fluxes to the interior of the Southern Ocean in the Western Pacific sector along 170° W, Deep-Sea Res. Pt. II, 47, 3521–3548, 2000.

Jickells, T. D., An, Z. S., Andersen, K. K., Baker, A. R., Bergametti, G., Brooks, N., Cao, J. J., Boyd, P. W., Duce, R. A., Hunter, K. A., Kawahata, H., Kubilay, N., laRoche, J., Liss, P. S., Mahowald, N., Prospero, J. M., Ridgwell, A. J., Tegen, I., and Torres, R.: Global iron connections between desert dust, ocean biogeochemistry, and climate, Science, 308, 67–71, 2005.

Klaas, C. and Archer, D. E.: Association of sinking organic matter with various types of mineral ballast in the deep sea: implications for the rain ratio, Global Biogeochem. Cy., 16, 1116, doi:10.1029/2001GB001765, 2002.

Lee, C., Peterson, M. L., Wakeham, S. G., Armstrong, R. A., Cochran, J. K., Miquel, J. C., Fowler, S. W., Hirschberg, D., Beck, A., and Xue, J.: Particulate organic matter and ballast fluxes measured using time-series and settling velocity sediment traps in the northwestern Mediterranean Sea, Deep-Sea Res. Pt. II, 56, 1420–1436, 2009.

de Mahiques, M. M., Coaracy Wainer, I. K., Burone, L., Nagai, R., de Mello e Sousa, S. H., Lopes Figueira, R. C., Almeida da Silveira, I. C., Bícego, M. C., Vicente Alves, D. P., and Hammer, Ø.: A high-resolution Holocene record on the Southern Brazilian shelf: paleoenvironmental implications, Quatern. Int., 206, 52–61, 2009.

Mahowald, N., Jickells, T. D., Baker, A. R., Artaxo, P., Benitez-Nelson, C. R., Bergametti, G., Bond, T. C., Chen, Y., Cohen, D. D., Herut, B., Kubilay, N., Losno, R., Luo, C., Maenhaut, W., McGee, K. A., Okin, G. S., Siefert, R. L., and Tsukuda, S.: Global distribution of atmospheric phosphorus sources, concentrations and deposition rates, and anthropogenic impacts, Global Biogeochem. Cy., 22, GB4026, doi:10.1029/2008gb003240, 2008.

Miquel, J. C., Fowler, S. W., La Rosa, J., and Buat-Menard, P.: Dynamics of the downward flux of particles and carbon in the open northwestern Mediterranean Sea, Deep-Sea Res. Pt. I, 41, 243–261, 1994.

BGD
11, 4909–4947, 2014

Mosseri, J., Quéguiner, B., Rimmelin, P., Leblond, N., and Guieu, C.: Silica fluxes in the north-east Atlantic frontal zone of Mode Water formation (38–45° N, 16–22° W) in 2001–2002, J. Geophys. Res., 110, C07S19, doi:10.1029/2004JC002615, 2005.

Neuer, S., Torres-Padroñ, M. E., Gelado-Caballero, M. D., Rueda, M. J., Hernañdez-Brito, J., Davenport, R., and Wefer, G.: Dust deposition pulses to the eastern subtropical North Atlantic gyre: does ocean's biogeochemistry respond?, Global Biogeochem. Cy., 18, GB4020, doi:10.1029/2004GB002228, 2004.

Paytan, A. and Kastner, M.: Benthic Ba fluxes in the central Equatorial Pacific, implications for the oceanic Ba cycle, Earth Planet. Sc. Lett., 142, 439–450, doi:10.1016/0012-821X(96)00120-3, 1996.

Ploug, H., Iversen, M. H., and Fisher, G.: Ballast, Sinking velocity, and apparent diffusivity within marine snow and zooplankton fecal pellets: implications for substrate turnover by attached bacteria, Limnol. Oceanogr., 53, 1878–1886, doi:10.4319/lo.2008.53.5.1878, 2008.

Putaud, J.-P., Van Dingenen, R., Dell'Acqua, A., Raes, F., Matta, E., Decesari, S., Facchini, M. C., and Fuzzi, S.: Size-segregated aerosol mass closure and chemical composition in Monte Cimone (I) during MINATROC, Atmos. Chem. Phys., 4, 889–902, doi:10.5194/acp-4-889-2004, 2004.

Ridame, C., Guieu, C., and L'Helguen, S.: Strong stimulation of N_2 fixation in oligotrophic Mediterranean Sea: results from dust addition in large in situ mesocosms, Biogeosciences, 10, 7333–7346, doi:10.5194/bg-10-7333-2013, 2013.

Ridame, C., Dekaezemacker, J., Guieu, C., Bonnet, S., L'Helguen, S., and Malien, F.: Phytoplanktonic response to contrasted Saharan dust deposition events during mesocosm experiments in LNLC environment, Biogeosciences Discuss., 11, 753–796, doi:10.5194/bgd-11-753-2014, 2014.

Schulz, M., Prospero, Baker, A. R., Dentener, F., Ickes, L., Liss, P. S., Mahowald, N. M., Nickovic, S., Perez, C., Rodriguez, S., Manmohan Sarin, M., Tegen, I., and Duce, R. A.: The atmospheric transport and deposition of mineral dust to the ocean: implications for research needs, Environ. Sci. Technol., 46, 10390–10404, doi:10.1021/es300073u, 2012.

Skonieczny, C., Bory, A., Bout-Roumazeilles, V., Abouchami, W., Galer, S. J. G., Crosta, X., Stuut, J. B., Meyer, I., Chiapello, I., Podvin, T., Chatenet, B., Diallo, A., and Ndiaye, T.: The 7–13 March 2006 major Saharan outbreak: multiproxy characterization of mineral dust deposited on the West African margin, J. Geophys. Res., 116, D18210, doi:10.1029/2011JD016173, 2011.

BGD
11, 4909–4947, 2014

Sullivan, R. C., Guazzotti, S. A., Sodeman, D. A., and Prather, K. A.: Direct observations of the atmospheric processing of Asian mineral dust, Atmos. Chem. Phys., 7, 1213–1236, doi:10.5194/acp-7-1213-2007, 2007.

Ternon, E., Guieu, C., Loÿe-Pilot, M.-D., Leblond, N., Bosc, E., Gasser, B., Miquel, J.-C., and Martín, J.: The impact of Saharan dust on the particulate export in the water column of the North Western Mediterranean Sea, Biogeosciences, 7, 809–826, doi:10.5194/bg-7-809-2010, 2010.

Wagener, T., Guieu, C., and Leblond, N.: Effects of dust deposition on iron cycle in the surface Mediterranean Sea: results from a mesocosm seeding experiment, Biogeosciences, 7, 3769–3781, doi:10.5194/bg-7-3769-2010, 2010.

Winckler, G., Anderson, R. F., and Schlosser, P.: Equatorial Pacific productivity and dust flux during the mid-Pleistocene climate transition, Paleoceanography, 20, PA4025, doi:10.1029/2005PA001177, 2005.

Wuttig, K., Wagener, T., Bressac, M., Dammshäuser, A., Streu, P., Guieu, C., and Croot, P. L.: Impacts of dust deposition on dissolved trace metal concentrations (Mn, Al and Fe) during a mesocosm experiment, Biogeosciences, 10, 2583–2600, doi:10.5194/bg-10-2583-2013, 2013.

BGD
11, 4909–4947, 2014

Table 1. Main operational details for seeding and sediment traps collection. The dust type is detailed in the Sect. 2.1 and hence e.g. EC Dust07 means evapocondensed dust collected in 2007.

	Dust seeding			Sediment traps collection			
	Date	Dust type	Added mass	Deposition type	First sample	Last sample	Average Resolution
DUNE-P	11–18 Jun 2008	EC-Dust07	41.5 g	Wet	Seeding + 24 h	Seeding + 168 h	48 h
DUNE-Q	20–27 Jun 2008	NEC-Dust07	41.5 g	Dry	Seeding + 24 h	Seeding + 168 h	48 h
DUNE-Rs1	27 Jun–3 Jul 2010	EC-Dust09	41.5 g	Wet	Seeding + 22 h	Seeding + 166 h	24 h
DUNE-Rs2	3–9 Jul 2010	EC-Dust09	41.5 g	Wet	Seeding + 24 h	Seeding + 144 h	24 h

BGD
11, 4909–4947, 2014

Table 2. Chemical composition of the fine fraction of soil (< 20 µm) used for different seedings.

	Experiment Q NEC Dust07	(±)	Experiment P EC Dust07	(±)	Experiment R EC Dust09	(±)
%Ca	18.62	**0.33**	17.95	**1.22**	16.54	**0.16**
%Si	15.16	**0.93**	13.59	**1.64**	11.94	**0.07**
%C	6.75	**0.01**	5.35	**0.06**	5.08	**0.02**
%Al	4.48	**0.12**	4.12	**0.39**	3.32	**0.03**
%Fe	2.28	**0.19**	2.31	**0.04**	2.26	**0.03**
%Mg	1.85	**0.17**	1.72	**0.28**	1.29	**0.02**
%K	1.19	**0.08**	1.15	**0.20**	0.96	**0.01**
%Ti	0.33	**0.03**	0.33	**0.03**	0.34	**0.01**
%N	0.11	**0.01**	1.19	**0.05**	1.36	**0.09**
%S	0.012	**0.001**	1.54	**0.01**	1.69	**0.02**
P (ppm)	442	**86**	454	**148**	552	**30**
Sr (ppm)	358	**23**	329	**39**	307	**27**
Mn (ppm)	354	**17**	354	**49**	342	**18**
Ba (ppm)	NA		NA		269	**14**
V (ppm)	NA		NA		58	**7.2**
Ni (ppm)	NA		NA		25	**1.1**
Cu (ppm)	15.0	**2.7**	15.5	**2.7**	16.4	**1.0**
Co (ppm)	11.0	**2.0**	8.4	**3.0**	8.8	**2.5**
Mo (ppm)	0.8	**0.3**	0.7	**0.2**	0.9	**0.1**
Li (ppm)	NA		NA		0.32	**0.01**
Nd (ppm)	NA		NA		0.19	**0.06**

NA: not available.

BGD
11, 4909–4947, 2014

Table 3. Total and elemental masses (mg) in the sediment traps of Control-Meso (samples xxC) and Dust-Meso (samples xxD) for the 4 seeding experiments: Q, P, R1 and R2.

Samples ID	Sampling time (h)	Total mass	C	N	Al	Ca	S
			Experiment P				
P1C	24	132 ± 86	30.0 ± 18.8	3.7 ± 2.2	3.1 ± 2.2	5.2 ± 3.2	1.0 ± 0.7
P2C	72	272 ± 191	59.1 ± 41.9	6.9 ± 5.5	9.0 ± 6.3	11.1 ± 7.2	1.0 ± 0.7
P3C	120	140 ± 122	33.7 ± 25.7	3.2 ± 2.8	2.4 ± 3.4	5.1 ± 6.0	0.8 ± 1.0
P4C	168	225 ± 210	17.2 ± 16.5	1.6 ± 1.5	1.2 ± 1.1	2.7 ± 2.5	0.5 ± 0.4
Cumulated mass		**769 ± 327**	**140.0 ± 12.8**	**15.4 ± 2.8**	**15.7 ± 3.2**	**24.1 ± 1.2**	**3.2 ± 0.5**
P1D	24	5051 ± 1458	350 ± 93	12.6 ± 1.2	234 ± 78	747 ± 260	29.4 ± 1.2
P2D	72	9092 ± 3008	633 ± 219	22.1 ± 7.2	443 ± 145	1340 ± 432	31.1 ± 12.2
P3D	120	3544 ± 1755	281 ± 153	11.9 ± 6.4	168 ± 86	499 ± 254	12.7 ± 7.2
P4D	168	788 ± 229	107 ± 22	8.8 ± 1.0	34 ± 11	93 ± 26	4.2 ± 1.2
Cumulated mass		**18 475 ± 1690**	**1372 ± 149**	**55.4 ± 6.9**	**881 ± 78**	**2679 ± 220**	**77.4 ± 13.4**
			Experiment Q				
Q1C	24	98 ± 54	22.9 ± 9.4	3.3 ± 1.0	2.2 ± 1.6	5.5 ± 3.5	0.6 ± 0.3
Q2C	73	92 ± 51	19.0 ± 10.8	2.3 ± 1.2	1.7 ± 1.4	4.1 ± 2.8	0.4 ± 0.3
Q3C	120	112 ± 15	24.2 ± 4.6	3.0 ± 0.7	2.5 ± 0.5	5.6 ± 0.6	0.7 ± 0.2
Q4C	168	146 ± 84	31.8 ± 18.7	3.7 ± 2.2	3.9 ± 2.8	6.9 ± 4.4	1.1 ± 0.7
Cumulated mass		**448 ± 165**	**97.9 ± 35.0**	**12.3 ± 4.0**	**10.4 ± 5.7**	**22.1 ± 8.6**	**2.8 ± 1.3**
Q1D	24	480 ± 198	53.0 ± 19.0	5.3 ± 2.3	22.2 ± 14.3	54.4 ± 33.6	2.4 ± 1.2
Q2D	73	781 ± 28	69.0 ± 3.2	4.4 ± 0.4	30.4 ± 8.8	73.8 ± 20.2	2.1 ± 0.6
Q3D	120	703 ± 260	66.7 ± 23.2	4.7 ± 1.5	24.7 ± 9.5	59.6 ± 21.9	1.8 ± 0.6
Q4D	168	368 ± 118	36.1 ± 11.2	2.8 ± 0.7	13.2 ± 4.4	31.1 ± 10.4	1.1 ± 0.4
Cumulated mass		**2332 ± 419**	**224.8 ± 38.3**	**17.2 ± 3.8**	**90.5 ± 30.4**	**218.8 ± 70.1**	**7.4 ± 2.2**
			Experiment R1				
R3C	22	276 ± 14	45.6 ± 3.6	3.7 ± 0.6	6.8 ± 1.3	16.7 ± 1.6	1.8 ± 0.5
R4C	46	285 ± 115	55.7 ± 23.8	5.6 ± 2.5	7.1 ± 3.7	12.2 ± 5.6	1.7 ± 1.0
R5C	70	173 ± 43	34.5 ± 7.5	3.6 ± 0.7	3.9 ± 0.9	5.3 ± 0.6	1.1 ± 0.3
R6C	94	168 ± 75	35.8 ± 15.7	4.0 ± 1.9	3.4 ± 1.2	4.1 ± 1.3	1.0 ± 0.4
R7C	118	89 ± 19	18.1 ± 4.0	2.1 ± 0.6	1.3 ± 0.2	2.5 ± 0.3	0.5 ± 0.1
R8C	142	38 ± 15	7.1 ± 3.4	0.8 ± 0.4	0.2 ± 0.1	0.4 ± 0.1	0.1 ± 0.0
R9C	166	68 ± 21	14.1 ± 3.5	1.7 ± 0.4	1.9 ± 0.7	5.4 ± 3.0	0.6 ± 0.3
Cumulated mass		**1096 ± 111**	**210.9 ± 22.6**	**21.5 ± 2.7**	**24.6 ± 1.5**	**46.7 ± 2.8**	**6.9 ± 0.6**
R3D	22	3890 ± 599	305 ± 37	12.8 ± 2.2	137 ± 29	496 ± 77	7.9 ± 1.9
R4D	46	5424 ± 956	385 ± 62	14.6 ± 3.3	199 ± 40	651 ± 98	10.1 ± 2.2
R5D	70	4193 ± 1012	314 ± 87	14.0 ± 4.6	182 ± 51	455 ± 106	10.0 ± 2.6
R6D	94	3784 ± 483	302 ± 39	16.9 ± 3.8	165 ± 21	557 ± 177	10.1 ± 1.9
R7D	118	1345 ± 513	112 ± 40	6.9 ± 1.7	59 ± 20	253 ± 201	4.2 ± 1.8
R8D	142	533 ± 98	47 ± 9	3.1 ± 0.8	19 ± 7	111 ± 97	1.4 ± 0.7
R9D	166	500 ± 228	51 ± 22	4.2 ± 1.6	19 ± 8	49 ± 8	1.6 ± 0.6
Cumulated mass		**19 669 ± 2757**	**1515 ± 229**	**72.6 ± 14.8**	**781 ± 118**	**2573 ± 628**	**45.3 ± 8.7**
			Experiment R2				
R11C	24	76 ± 11	16.9 ± 2.2	2.1 ± 0.2	2.4 ± 0.3	5.9 ± 1.6	0.7 ± 0.1
R12C	48	50 ± 15	11.2 ± 2.7	1.4 ± 0.3	1.0 ± 0.5	4.2 ± 3.8	0.4 ± 0.3
R13C	72	58 ± 7	12.2 ± 3.2	1.4 ± 0.3	1.2 ± 0.0	7.7 ± 2.5	0.4 ± 0.1
R14C	96	23 ± 23	4.0 ± 4.0	0.6 ± 0.6	0.3 ± 0.3	3.0 ± 3.0	0.3 ± 0.3
R15C	120	19 ± 19	3.4 ± 3.4	0.4 ± 0.4	0.3 ± 0.3	1.8 ± 1.8	0.2 ± 0.2
R16C	144	19 ± 19	4.0 ± 4.0	0.6 ± 0.6	0.2 ± 0.2	1.9 ± 1.9	0.2 ± 0.2
Cumulated mass (mg)		**245 ± 24**	**51.8 ± 5.6**	**6.3 ± 0.6**	**5.3 ± 0.8**	**24.6 ± 2.4**	**2.2 ± 0.2**
R11D	24	4461 ± 517	323 ± 31	14.9 ± 2.6	161 ± 54	566 ± 148	8.6 ± 3.1
R12D	48	2836 ± 520	200 ± 42	12.3 ± 2.8	119 ± 21	386 ± 70	6.2 ± 1.2
R13D	72	3456 ± 1348	249 ± 97	12.6 ± 3.5	145 ± 67	496 ± 230	8.4 ± 3.0
R14D	96	677 ± 254	54 ± 18	3.0 ± 0.9	24 ± 11	87 ± 38	1.3 ± 0.6
R15D	120	352 ± 233	31 ± 22	2.1 ± 1.7	13 ± 9	48 ± 31	1.1 ± 0.8
R16D	144	181 ± 120	19 ± 12	1.8 ± 1.1	6 ± 4	24 ± 16	0.7 ± 0.4
Cumulated mass (mg)		**11 962 ± 2117**	**876 ± 151**	**46.7 ± 7.2**	**467 ± 98**	**1608 ± 260**	**26.4 ± 3.9**

BGD
11, 4909–4947, 2014

Table 4. Enrichment factors $(X/Al)_{sediment}/(X/Al)_{dust}$ in the material collected in the sediment traps of the Dust-Meso for the 4 DUNE experiments.

Exp.	C	N	Ba	Ca	Co	Cu	Fe	Li	Mn	Mo	Nd	P	S	Sr	Ti
Q	1.62	7.32		0.58	1.18	1.26	0.99		0.75			2.91		0.88	1.01
P	1.14	0.19		0.70	1.67	1.32	0.99		0.72			1.09	0.22	0.76	0.96
R1	1.24	0.22	0.93	0.63	1.95	2.21	1.04	1.08	0.94	1.08	0.96	1.27	0.11	1.03	1.02
R2	1.19	0.24	1.02	0.69	1.92	1.18	1.08	1.13	0.94	0.86	0.97	1.23	0.11	1.01	1.09

BGD
11, 4909–4947, 2014

Table 5. Mass budget in sediment traps: the dissolved mass of dust corresponds to the dissolved mass of $CaCO_3$ for the Q experiment and of $CaSO_4$and $Ca(NO_3)_2$ for P, R1 and R2 experiments, estimated from the S, N and Ca contents measured in sediment traps.

Experiments	Total mass (mg) measured (±)	Estimated from Al	Dissolved mass of dust (mg)	% dissolved mass	Estimated mass from Al corrected of the dissolved mass (mg)	Total dissolved mass for initial dust (mg)	% of dust in total mass
Q	2332 ± **419**	2019	265	13 %	1 755	6296	75 %
P	18 474 ± **1690**	21 373	4209	20 %	17 165	6412	93 %
R1	19 669 ± **2757**	23 557	4816	20 %	18 741	7322	95 %
R2	11 962 ± **2123**	14 067	2616	19 %	11 451	7213	96 %

BGD
11, 4909–4947, 2014

Table 6. Integrated POC, lithogenic, opal and biogenic $CaCO_3$ mass fluxes ($mg\,m^{-2}\,d^{-1}$) determined from mass in sediment traps for the 4 seeding experiments.

		P	Q	R1	R2
POC flux	control	4.3 ± 3.2	2.8 ± 1.3	6.8 ± 4.3	1.6 ± 1.2
	dust	21.9 ± 11.8	5.0 ± 2.5	17.1 ± 10.0	10.9 ± 9.7
	ratio	**5.1**	**1.8**	**2.5**	**6.8**
Lithogenic flux	control	6.3 ± 7.0	4.4 ± 2.5	8.0 ± 6.4	2.5 ± 2.4
	dust	646 ± 499	63.7 ± 21.9	565 ± 392	359 ± 341
	ratio	**103**	**14**	**71**	**144**
Opal flux	control	1.5 ± 1.4	1.0 ± 0.7	13 ± 13	1.4 ± 0.4
	dust	30 ± 24	2.4 ± 0.7	12 ± 22	19 ± 65
	ratio	**19**	**2**	**1**	**14**
$CaCO_3$bio flux	control	< DL	0.2 ± 0.1	1.0 ± 2.5	1.46 ± 1.1
	dust	28 ± 29	6.7 ± 2.5	98.1 ± 74	61 ± 56
	ratio		**34**	**94**	**42**
Litho/POC	control	1.5	1.6	1.2	1.6
	dust	29.5	12.8	33.1	32.9

BGD
11, 4909–4947, 2014

Table 7. Average of integrated elemental mass fluxes ($mg\,m^{-2}\,d^{-1}$) determined from the elemental masses in sediment traps of Control-Meso and Dust-Meso for the 4 DUNE experiments P, Q, R1 and R2.

		N	(±)	Al	(±)	Ba	(±)	Co	(±)	Cu	(±)	Fe	(±)
control	P	0.6	**0.3**	0.6	**0.4**	0.004	**0.004**	0.0004	**0.0003**	0.001	**0.001**	0.4	**0.3**
	Q	0.5	**0.2**	0.4	**0.2**	0.002	**0.001**	0.0001	**0.0000**	0.0003	**0.0001**	0.2	**0.1**
	R1	0.8	**0.4**	0.9	**0.7**	0.007	**0.005**	0.0003	**0.0002**	0.056	**0.040**	0.5	**0.4**
	R2	0.3	**0.2**	0.2	**0.2**	0.001	**0.001**	0.0001	**0.0001**	0.0004	**0.0003**	0.1	**0.1**
dust	P	2.0	**0.9**	33.6	**25.5**	0.14	**0.11**	0.013	**0.010**	0.018	**0.015**	51.9	**34.2**
	Q	0.7	**0.4**	3.4	**1.6**	0.03	**0.01**	0.001	**0.000**	0.001	**0.001**	1.7	**0.8**
	R1	2.5	**1.4**	27.3	**18.8**	0.20	**0.14**	0.014	**0.010**	0.028	**0.026**	53.1	**34.9**
	R2	1.9	**1.5**	18.7	**17.1**	0.15	**0.14**	0.010	**0.009**	0.011	**0.010**	35.2	**31.0**
		Li	(±)	Mn	(±)	Mo	(±)	Nd	(±)	P	(±)	Ti	(±)
control	P	0.004	**0.003**	0.005	**0.003**	0.001	**0.001**	0.002	**0.001**	0.10	**0.04**	0.05	**0.04**
	Q	0.004	**0.001**	0.002	**0.001**	0.0003	**0.0001**	0.000	**0.000**	0.09	**0.03**	0.03	**0.01**
	R1	0.0001	**0.0002**	0.009	**0.007**	0.00005	**0.00004**	0.004	**0.002**	0.04	**0.02**	0.05	**0.04**
	R2	0.0002	**0.0002**	0.002	**0.001**	0.00001	**0.00001**	0.001	**0.001**	0.02	**0.01**	0.01	**0.01**
dust	P	0.134	**0.097**	0.24	**0.20**	0.034	**0.025**	0.07	**0.05**	0.4	**0.3**	2.6	**2.0**
	Q	0.006	**0.002**	0.02	**0.01**	0.004	**0.002**	0.003	**0.002**	0.1	**0.1**	0.3	**0.1**
	R1	0.029	**0.020**	0.26	**0.19**			0.12	**0.08**	0.6	**0.4**	2.9	**2.0**
	R2	0.021	**0.019**	0.18	**0.17**			0.08	**0.08**	0.4	**0.3**	2.1	**1.9**

BGD
11, 4909–4947, 2014

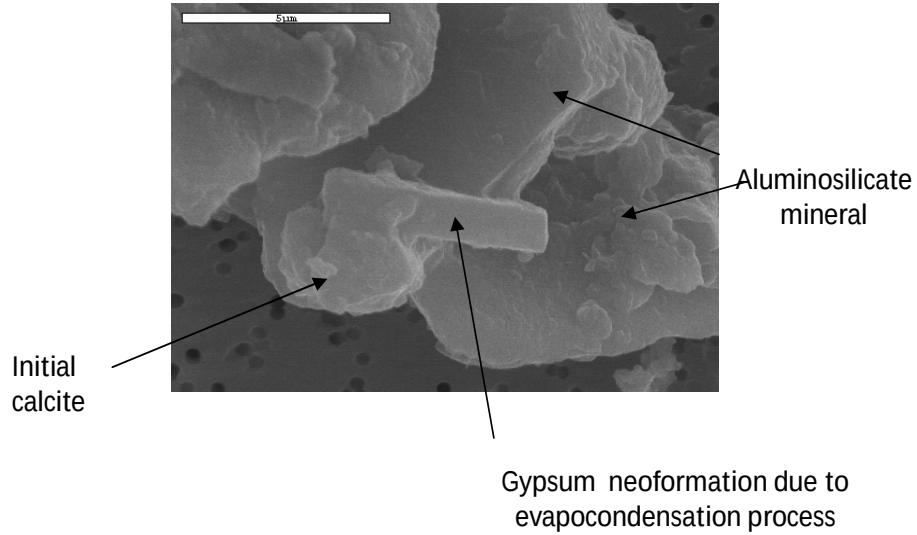

Fig. 1. Electronic microscope image of neoformation of gypsum ($CaSO_4$) from initial calcite ($CaCO_3$) mixed with sulfuric acid during cloud processing simulation.

BGD
11, 4909–4947, 2014

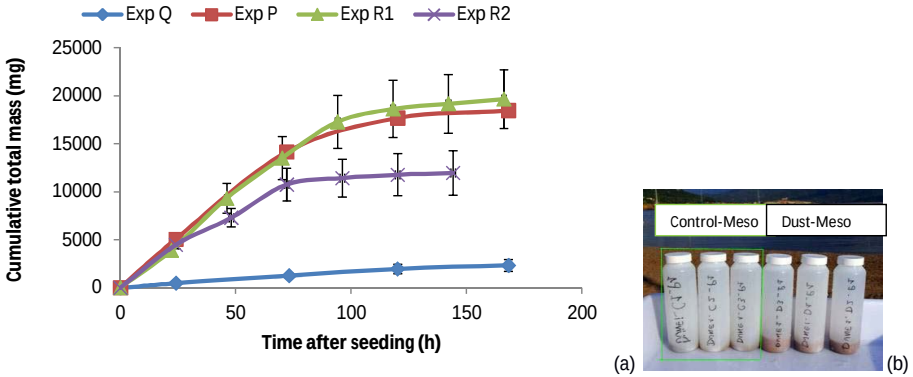

Fig. 2. (a) Cumulative total mass as a function of time after seeding in the Dust-Meso sediments traps for the 4 experiments and **(b)** picture of collected mass in the sampling bottles of sediment traps for the experiment P 24 h after seeding.

BGD
11, 4909–4947, 2014

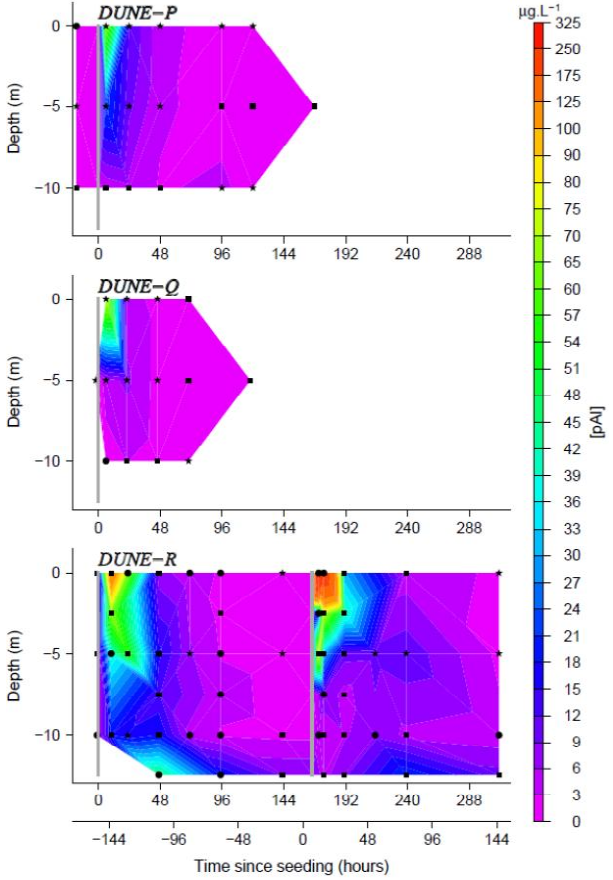

Fig. 3. Temporal evolution of particulate aluminium concentrations in the Dust-Meso for the four seedings. Stars represent the points where the average mesocosms concentration of three replicated mesocosms is used, triangles two replicated mesocosms and circles only one mesocosm. The grey vertical bars highlight the time points when the seeding took place.

BGD
11, 4909–4947, 2014

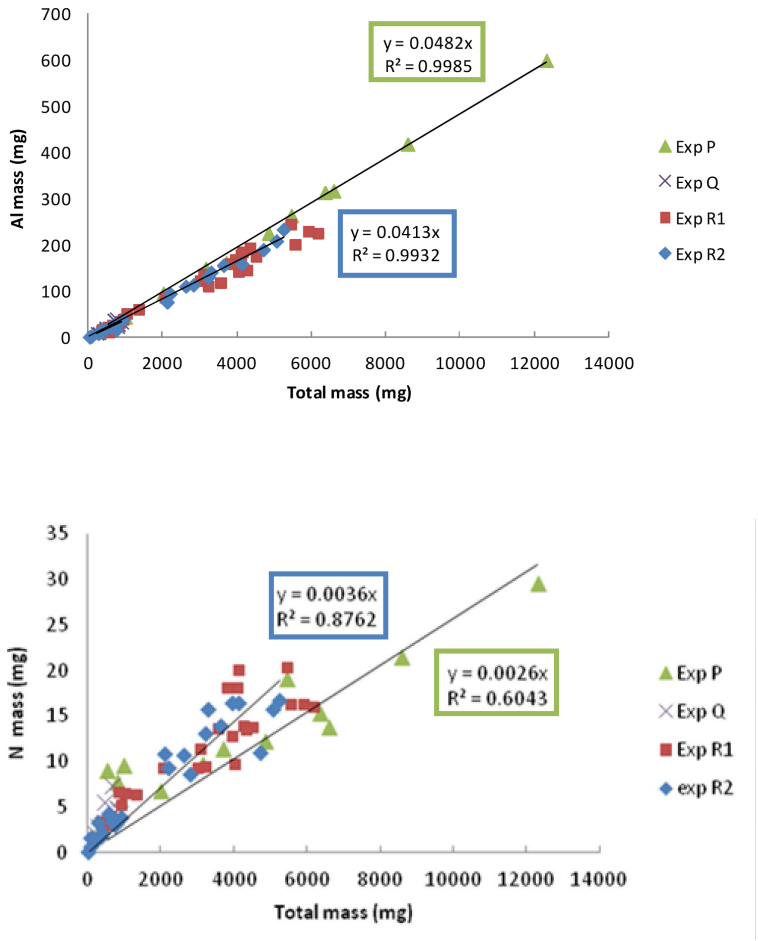

Fig. 4. Al and N mass vs. total mass in each sediment trap of all the samples of the Dust-Meso for the 4 experiments and linear regression for experiments P and R2.

BGD
11, 4909–4947, 2014

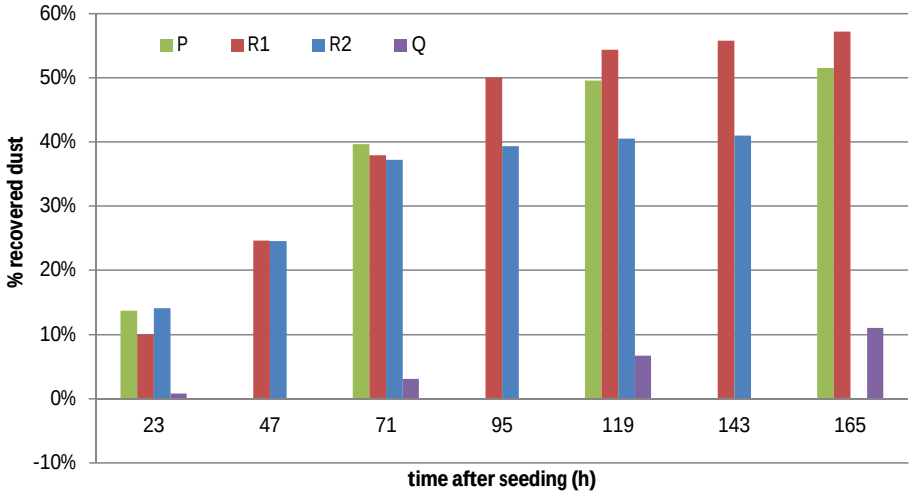

Fig. 5. Mass percentage of recovered dust in the sediment traps in comparison to the added mass at t_0 considering the dissolution of evaporite species for the experiments P, R1 and R2 as a function of time after seeding.

BGD
11, 4909–4947, 2014